

PAPER • OPEN ACCESS

## Tetrahedral intrinsic structure of Oxygen-16 revisited

To cite this article: C J Halcrow and N S Manton 2020 *J. Phys.: Conf. Ser.* **1643** 012136

View the [article online](#) for updates and enhancements.



The banner features a decorative top border with a repeating pattern of red, white, and blue diagonal stripes. On the left, the ECS logo is displayed in green and blue, followed by the text 'The Electrochemical Society' and 'Advancing solid state & electrochemical science & technology'. To the right of this text is a logo for the 18th International Meeting of the Chemical Society of Japan (IMCS18), consisting of a stylized 'E' and 'C' with '18th' below it. The main text of the banner reads '239th ECS Meeting with IMCS18' in large blue font, followed by 'DIGITAL MEETING • May 30-June 3, 2021' and 'Live events daily • Free to register' in black font. On the right side, there is a graphic showing a person's face overlaid with a digital network of nodes and lines, with a laptop icon below it. A red button with white text 'Register now!' is positioned at the bottom right of the banner.

**ECS** The Electrochemical Society  
Advancing solid state & electrochemical science & technology

**239th ECS Meeting with IMCS18**

DIGITAL MEETING • May 30-June 3, 2021

Live events daily • Free to register

Register now!

# Tetrahedral intrinsic structure of Oxygen-16 revisited

C J Halcrow<sup>1</sup> and N S Manton<sup>2</sup>

<sup>1</sup> School of Mathematics, University of Leeds, Leeds LS2 9JT, U.K.

<sup>2</sup> Department of Applied Mathematics and Theoretical Physics, University of Cambridge, Wilberforce Road, Cambridge CB3 0WA, U.K.

E-mail: c.j.halcrow@leeds.ac.uk, N.S.Manton@damtp.cam.ac.uk

**Abstract.** A model for vibrational and rotational excitations of an intrinsic tetrahedral structure of the Oxygen-16 nucleus has been investigated, building on classic work of Wheeler, Dennison and Robson. Tetrahedral A- and F-phonons are treated harmonically, but the E-phonon dynamics is extended to dynamics on an E-manifold of configurations of four  $\alpha$ -particles. This allows for tunnelling between the tetrahedral configuration and its dual, through a square configuration, and lifts the parity doubling that would otherwise occur. Unlike in earlier models, including the algebraic cluster model, the E-phonon frequency is taken to be about half the F-phonon frequency, which in turn is about half the A-phonon frequency. As a result, the first-excited  $0^+$  state is a 2-phonon, E-manifold excitation, whereas the lowest  $2^+$  and  $2^-$  states are 1-phonon, E-manifold excitations. Coriolis contributions to the rotational energy of states with F-phonons are significant. Altogether, rotational bands are constructed based on vibrational states with up to four phonons, and with spin/parity up to  $9^-$ . Nearly all the observed states of Oxygen-16 are accommodated, up to 20 MeV and partly beyond. Predictions for some so far unobserved states, especially those of unnatural parity, are made.

## 1. Introduction

In 1937, Wheeler showed that several properties of nuclei with atomic mass number  $4N$  and equal numbers of protons and neutrons could be explained using an  $\alpha$ -particle model [1]. According to Wheeler, such a nucleus is a molecule of  $N$   $\alpha$ -particles. Our interest is in Oxygen-16, a molecule of four  $\alpha$ -particles sitting on the vertices of a tetrahedron, and we have recently investigated its energy spectrum by considering the motion of the tetrahedron. Quantized rigid rotations lead to a rotational band having spin/parities  $0^+, 3^-, 4^+, \dots$ . The  $\alpha$ -particles can also move relative to one another, causing the tetrahedron to deform. Such motions are known as vibrational modes. They lead to vibrational states in the energy spectrum, together with further rotational excitations. The spins and energies crucially depend on the symmetries and frequencies of these classical vibrations.

The tetrahedral structure also arises in the Skyrme model. The Skyrme model is a nonlinear theory of pions where nuclei are described as quantized, topologically non-trivial knots in the pion field, known as Skyrmions [2]. The topological charge of a Skyrmion is its baryon number (atomic mass number)  $B$ . In practice, one can think of a Skyrmion as a localised lump of energy. The  $B = 16$  Skyrmion models  $^{16}\text{O}$  and its energy density is indicated in the middle column of Figure 1, with the colouring capturing aspects of the field values. It has tetrahedral symmetry and can be interpreted as four  $\alpha$ -particles, as is evident from the Figure. Skyrmion dynamics is



baked into the theory and so understanding the vibrational modes of the tetrahedron is relatively straightforward.

## 2. Vibrations and vibrational wavefunctions

There are three low-frequency vibrational modes associated with  $\alpha$ -particle motion. They are labeled by the irreducible representations of the tetrahedral group: A, E and F. A particular motion in each of the vibrational spaces is shown in Figure 1, as well as a description of each mode. One can calculate the frequencies of the modes in the Skyrme model. The results suggest that the E-frequency is much lower than the others, so the E-vibration should be treated with care. The E-vibration is important for a second reason: it links the tetrahedral configuration to the square configuration. The square consists of four  $\alpha$ -particles on the vertices of a flat square. A motion linking the tetrahedron to the square is shown in Figure 2. The square has low energy, just above that of the tetrahedron, and a large symmetry group. Hence its existence can affect the  $^{16}\text{O}$  energy spectrum, as we shall see.

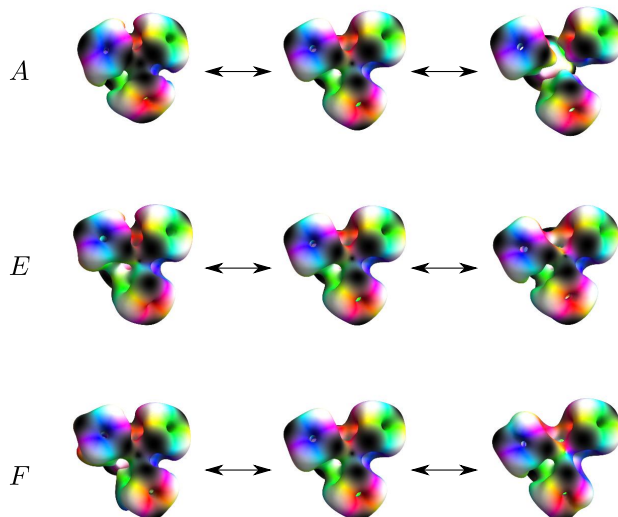


**Figure 1.** The A-, E- and F-vibrational modes. The A-vibration corresponds to all particles moving in and out, preserving tetrahedral symmetry. In one direction of the two-dimensional E-vibration, the top and bottom pairs of particles move towards and away from each other. In the F-vibration, one particle moves away from the other three, which form an equilateral triangle. Other choices of direction in each vibrational space can be made, such as Wheeler describing the E-vibration as a “twisting” motion [1]. This alternative interpretation is simply a choice of basis used for visualisation, and has no effect on the final calculation.

Using methods detailed in [3, 4], we can parameterise configurations in the E-vibrational space using a portion of the plane. We call this two-dimensional manifold of configurations the E-manifold,  $\mathcal{M}_E$ . It includes the tetrahedral and square configurations, as well as all those

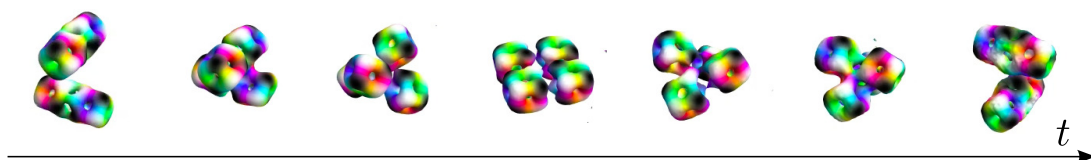


**Figure 2.** A dynamical path joining tetrahedral and square configurations. Initially two  $B = 8$  Skyrmions are sent towards one another. They form the tetrahedron, then continue on, flattening out and becoming the square. Their momentum then carries them into the dual tetrahedron before the two  $B = 8$  Skyrmions appear again and fly out to infinity. All of these configurations are contained in the E-manifold.

joining them and more. It is plotted in Figure 3, where we have highlighted the locations of the squares and tetrahedra. We must now solve the Schrödinger equation on  $\mathcal{M}_E$  to obtain vibrational wavefunctions. In a standard cluster model, these would be harmonic wavefunctions with energies  $\hbar\omega_E(n + 1/2)$  and  $n$  counting the number of E-phonons. The phonon concept still applies in the E-manifold, as it characterises each wavefunction close to one of the tetrahedra, and hence we can label the wavefunctions using the integer  $n$ . However, the wavefunctions and energies differ significantly compared to the harmonic approximation. We display the ground (or 0-phonon) state, a 1-phonon state and a 2-phonon state in Figure 3. The 0-phonon state is concentrated at the tetrahedra, while the 1-phonon state is concentrated at the squares. The 2-phonon state is more interesting, as it is concentrated around both types of configuration, so physically, it superposes square and tetrahedral configurations.

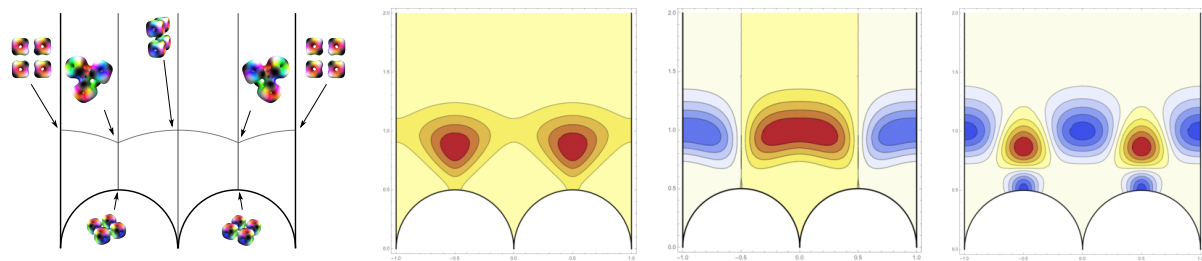


**Figure 3.** The E-manifold and some vibrational wavefunctions on it. The E-manifold is contained within the thick black lines of the leftmost figure. The regions where the wavefunction is concentrated are shown red (positive) and blue (negative). The three vibrational wavefunctions are 0-, 1- and 2-phonon states respectively.

### 3. Physical states

To create physical states, we must combine the vibrational wavefunctions with spin states, which describe the rigid rotations of the nucleus. We also include harmonic A- and F-vibrations. The allowed combinations are determined by the symmetry of the system. The calculation is standard in molecular chemistry and classic textbooks such as [5] are of great assistance. The Hamiltonian of an allowed state is given by

$$\mathcal{H} = E_{vib} + \hbar\omega_F(n_F + 1/2) + \hbar\omega_A(n_A + 1/2) + \hbar^2 B(\hat{J} - \zeta\hat{l})^2 + C(J(J+1))^2 + D(J(J+1))^3, \quad (1)$$

where  $E_{vib}$  is the energy of the underlying vibrational wavefunction on  $\mathcal{M}_E$ ,  $\omega_F$  and  $\omega_A$  are the frequencies of the F- and A-vibrations, and  $n_F$  and  $n_A$  are the number of F- and A-phonons. We take  $\omega_A \approx 2\omega_F$ . Although we do not have a harmonic E-vibration, we can calculate an effective  $\omega_E$  using the energies of the 1- and 2-phonon states on the E-manifold. We find that  $\omega_E \approx \omega_F/2$ . Our values are in sharp contrast to [8], where all vibrations have the same frequency. The remainder of (1) is a rotational contribution.  $\hat{J}$  is the spin operator while  $\hat{l}$  is the orbital angular momentum of the F-phonons. The coefficient  $B$  (here, not the baryon number) is related to the moment of inertia of the nucleus while  $C$  and  $D$  control the centrifugal corrections. Finally,  $\zeta$  is the strength of the Coriolis correction. Apart from our careful treatment of the E-vibration, the main difference from previous work is our value of  $\zeta$ . Robson and Dennison use  $\zeta = 0.5$ , a value taken from the point-particle world of molecular physics [6, 7]. Our  $\alpha$ -particles have structure and so the value should be different. Hence we treat  $\zeta$  as a parameter and fix it to  $-0.2$ . This could be checked in the Skyrme model numerically.

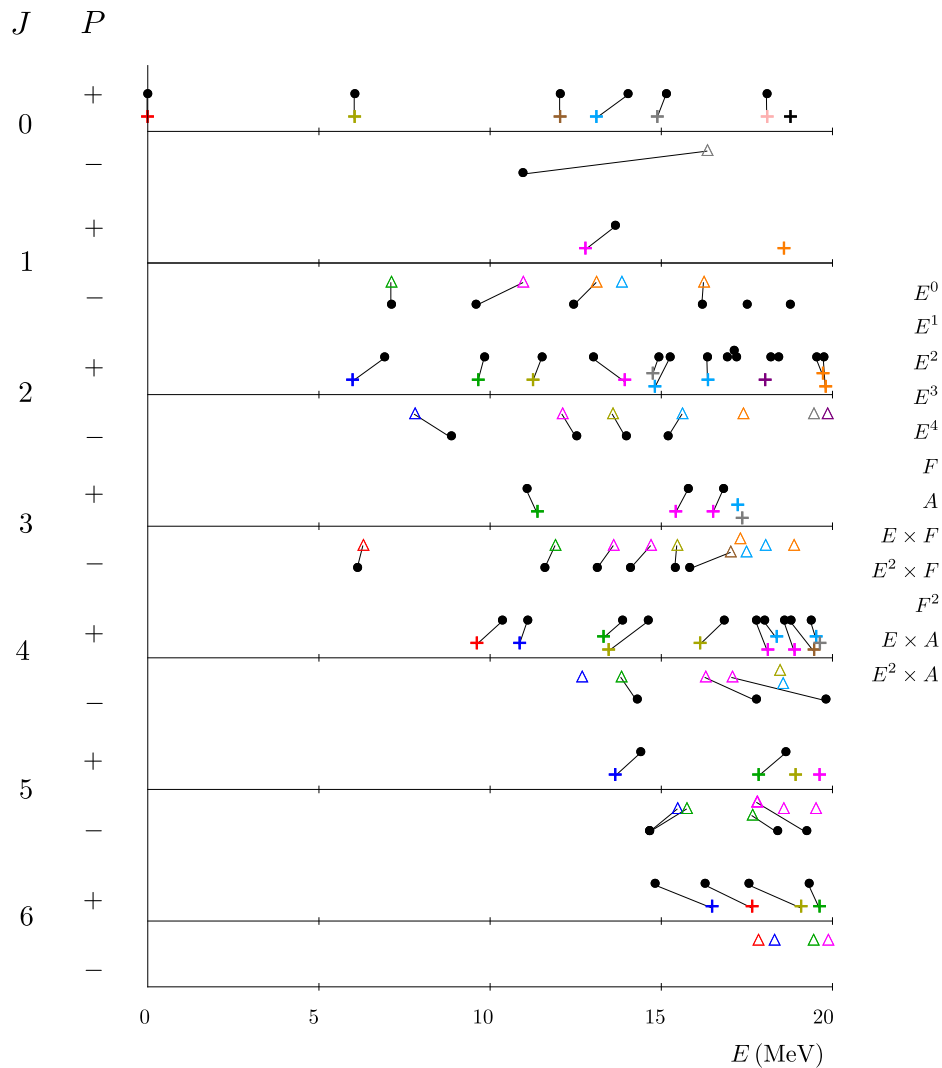


**Figure 4.** Comparison between theoretical and experimental energies. Positive (negative) parity states of our model are displayed as pluses (triangles), and coloured according to their number of phonon excitations in each vibrational mode. Experimental states are displayed as black dots. Our identifications between theoretical and experimental states are shown by lines joining the states.

#### 4. Comparison to experiment

The results of our calculation of the  $^{16}\text{O}$  spectrum are shown in Figure 4. Coloured symbols and black dots represent, respectively, states in our theoretical model and experimental states. The different colours represent the different types of state. For example, the rotational band of states with one F-phonon and one E-phonon is coloured bright pink, as indicated in the key. When we believe that there is a match between experimental and model states, we draw a line between them. We plot around 60 states and almost all are easy to match up.

Our model reproduces aspects of a simple tetrahedral model, including a ground-state rotational band with spin/parities  $0^+, 3^-, 4^+, \dots$ . These states all use the 0-phonon vibrational wavefunction in their construction. In contrast to a simple tetrahedral model, there is a 2 MeV gap between the lowest-lying spin 2 states, with positive and negative parity. This is due to

the existence of the square configuration. The negative parity state is forced to vanish at the square, as the geometry of the square only allows positive parity. This means that the  $2^-$  vibrational wavefunction is more constrained than the  $2^+$  one. Generally, the more constrained a wavefunction is, the higher its energy. This is the case here, as is explained in detail in [3, 4]. This gap is not present in models where fluctuations are small, such as [8].

Experimentally, the first excited state has spin/parity  $0^+$ , which is very unusual. In our model, this state is a 2-phonon excitation whose underlying E-manifold wavefunction is shown on the right of Figure 3. It is concentrated not just on a tetrahedral or square configuration, but superposes both. Our model also reproduces the large gaps in the spectrum between the unnatural parity  $2^-$  states and  $3^+$  states. The main prediction of the model is an additional  $4^-$  state below 15 MeV. One such state has already been observed and experimentally it may be hard to disentangle two states. We also predict many high-spin, unnatural-parity states (not shown in Figure 4, but present in [3, 4]). The biggest disparity between model and experiment is the  $0^-$  state. Its energy in our model is much too large. However, this type of state is difficult to construct in many models, including the shell model. In fact, this is the first ever isospin 0, spin/parity  $0^-$  state to be constructed in the Skyrme model. We hope that future work can bring the energy down, without affecting the many successes of the model.

## 5. Future work

There are two obvious next steps: to study this model in more detail and refine it, and to try and apply the ideas to larger nuclei. We hope to soon tackle the former by calculating electromagnetic transition rates in this model. These depend crucially on the structure of the wavefunctions and their overlap. As our vibrational wavefunctions are rather unique, we should obtain equally unique results for the electromagnetic transitions. Moving up the nuclear chart, the next suitable  $\alpha$ -particle nucleus is Neon-20. In the past, authors have modelled this by arranging the  $\alpha$ -particles into a trigonal bipyramid, though comparison with experiment was poor [9]. The Skyrme model can be used to find the low energy configurations of significance, analogous to the tetrahedron and square here. Including low frequency vibrational modes, possibly extended into a nonlinear manifold, again as here, could improve the results for Neon-20.

## Acknowledgements

CJH is supported by The Leverhulme Trust as an Early Careers Fellow. NSM's work has been partially supported by STFC consolidated grant ST/P000681/1.

## References

- [1] J. A. Wheeler, Molecular viewpoints in nuclear structure. *Phys. Rev.* **52** (1937) 1083.
- [2] T. H. R. Skyrme, A non-linear field theory. *Proc. Roy. Soc. Lond. A* **260** (1961) 127.
- [3] C. J. Halcrow, C. King and N. S. Manton, Dynamical  $\alpha$ -cluster model of  $^{16}\text{O}$ . *Phys. Rev. C* **95** (2017) 031303(R).
- [4] C. J. Halcrow, C. King and N. S. Manton, Oxygen-16 spectrum from tetrahedral vibrations and their rotational excitations. *Int. J. Mod. Phys. E* **28**, **04** (2019) 1950026.
- [5] G. Herzberg, *Molecular Spectra and Molecular Structure: II. Infrared and Raman Spectra of Polyatomic Molecules*. Van Nostrand, Princeton NJ, 1945.
- [6] D. M. Dennison, Excited states of the  $\text{O}^{16}$  nucleus. *Phys. Rev.* **57** (1940) 454; Energy levels of the  $\text{O}^{16}$  nucleus. *Phys. Rev.* **96** (1954) 378.
- [7] D. Robson, Evidence for the tetrahedral nature of  $^{16}\text{O}$ . *Phys. Rev. Lett.* **42** (1979) 876; Test of tetrahedral symmetry in the  $^{16}\text{O}$  nucleus. *Phys. Rev. C* **25** (1982) 1108.
- [8] R. Bijker and F. Iachello, Evidence for tetrahedral symmetry in  $^{16}\text{O}$ . *Phys. Rev. Lett.* **112** (2014) 152501.
- [9] D. M. Brink, H. Friedrich, A. Weiguny and C. W. Wong, Investigation of the alpha-particle model for light nuclei. *Phys. Lett. B* **33** (1970) 143.